

Forced Convection Heat Transfer in the Entrance Region of Horizontal Tube under Constant Heat Flux

S.M. Peyghambarzadeh

Department of Chemical Engineering, Mahshahr Branch, Islamic Azad University, Mahshahr, Iran

Abstract: The presence of free convection in the fully turbulent flow forced convection has been studied experimentally in the thermal entry of horizontal tube. Tube wall was subjected to constant heat flux boundary condition varied in two levels 1300 and 3000 W/m². Some thermocouples installed along the tube length to measure the temperature data and these were used to calculate local heat transfer coefficients and local Nu numbers in the test section. Results demonstrated that higher Nu numbers were recorded in the initial parts of the tube. Also, it was presented that Nu number distribution at higher heat flux condition is slightly greater than that of lower heat flux at similar Re numbers. This effect was related to the secondary flow induced by buoyancy force which manifests itself at higher heat flux and lower flow rates. It can be concluded that even in the turbulent flow forced convection, the effect of free convection cannot be neglected. Meanwhile, the present study simulates the performance of a mixed convection heat transfer using FLUENT code. Results show that the predictions of numerical method are in good agreement with the experimental data.

Key words: Forced and free convection • Horizontal tube • Experimental • Heat transfer coefficient

INTRODUCTION

Pure forced convective heat transfer seldom occurs in reality since the density of ordinary fluids is dependent on temperature. In fact, mixed convection, that is, combined free and forced convection, is the most general type of phenomena. Pure forced or pure free convection are only the limiting cases when either type of mixing motion can be neglected in comparison to the other. Application of heat to the tube wall produces a temperature difference in the fluid. The fluid near the tube wall has a higher temperature and lower density than the fluid close to the centerline of the tube. This temperature difference may produce a secondary flow due to free convection. Mixed convection heat transfer, in addition to being dependent on Reynolds and Prandtl numbers, is also dependent upon the Grashof number which accounts for the variation in density of the test fluid [1]. Faris and Viskanta [2] showed that there are no appreciable free convection effects in the thermal entrance region. Also, it was emphasized by Tam and Ghajar [3] that for turbulent flow, buoyancy has little effect on the velocity and temperature fields (liquid metals being excepted). Therefore, it is expected that the secondary flow effect is suppressed by the turbulent

motion and the heat transfer mode is pure forced convection.

Various experimental, numerical and analytical studies are available for forced and mixed convection heat transfer in horizontal tubes with a rounded entrance in the laminar, transitional and turbulent flow regimes. Mori *et al.* [4] carried out experiments to study the effect of buoyancy force on forced convection for fully developed air flow under constant wall heat flux. The calculated Nusselt number was also shown to be twice as those calculated by neglecting the effect of secondary flow. Kopper *et al.* [5] presented experimental results of the effect of free convection on forced convection in a horizontal circular tube with uniform heat flux at the wall. Water was used as the working medium. The results indicated appreciable increase in the Nusselt number. Lei and Trupp [6] investigated experimentally combined convection for laminar water flow in the entrance region of a horizontal semicircular duct with uniform heat input axially. Measurements were made of axial and circumferential wall temperature variations together with pressure drops across the heated section in order to study the effects of the buoyancy-induced secondary flow. Recently, Mohammed *et al.* [7] studied the interaction of free and

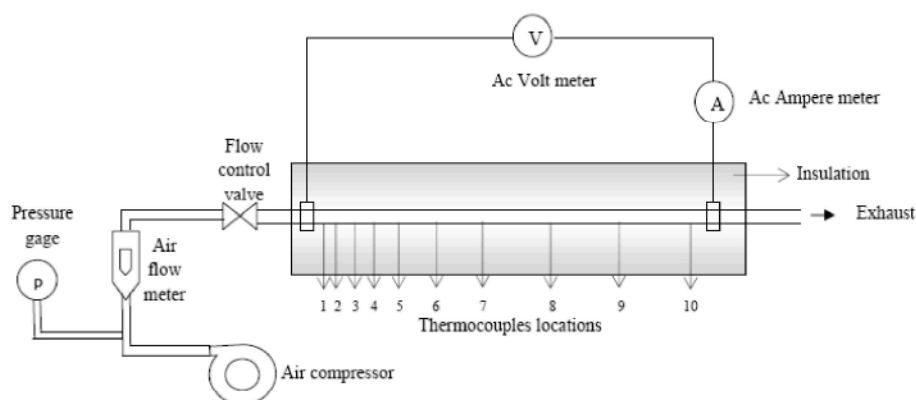


Fig. 1: Simplified diagram of experimental apparatus

forced convection in an annulus in laminar flow condition ($200 < Re < 1000$) and concluded that free convection effects tended to decrease the heat transfer at low Re number while to increase the heat transfer at high Re number.

As shown in the previous literatures, the effects of secondary flow due to buoyancy force on laminar forced convection have been studied by several investigators but its effect on turbulent flow forced convection were analyzed with less details and almost no experimental works were found about it in the literature. The objective of this study was to experimentally investigate the behavior of local heat transfer coefficient in the turbulent flow regime for a circular tube. For this purpose, local heat transfer measurements under uniform wall heat flux boundary condition were made at different levels of heat flux and air flow rate at the entry section of a horizontal tube.

Experimental Set up: Figure 1 shows the experimental apparatus used in this study. It consisted of a stainless steel tube as a part of an open-air circuit, with inner diameter of 5 mm and outer diameter of 6 mm. There are 11 thermocouples along the length of the tube from fluid entrance to exit. Outside wall temperatures are read with these digital thermocouples. The locations of thermocouples have been shown in Table 1. As can be seen in Table 1, the distances between thermocouples have been increased as fluid reaches to the end of the tube. This is due to the sharp temperature variation occurs at the entrance of the tube and at the initial contact of fluid with tube wall. Direct ohmic heating in the tube wall is employed to give a uniform wall heat flux to the air. The outside wall of the tube is heavily insulated giving essentially zero heat loss to the surroundings. The power supply to the electrical heater can be calculated by reading of voltage and current applied as follow:

Table 1: The locations of the thermocouples along the tube length

Thermocouples	Distance from the beginning (mm)
T_{in}	0
T_1	5
T_2	10
T_3	20
T_4	30
T_5	50
T_6	100
T_7	200
T_8	400
T_9	600
T_{10}	800

Table 2: Some characteristics of the experimental set up used in this study

Quantity	Value
Internal diameter of the tube	5 mm
external diameter of the tube	6 mm
Tube thickness	0.5 mm
Tube Material	Stainless steel
Thermocouple material	Chromel-alumel
Tube length	900 mm
Tube thermal conductivity	16.28 W/m °C
Insulator thickness	50 mm
Insulator thermal conductivity	0.043 W/m °C
AC Volt meter	0 to 5 V
AC Amper meter	0 to 70 A

$$q = VI \quad (1)$$

High pressure air from compressor is used as air source. The air volume flow rate was measured with the flow meter which was installed at the entrance of the tube. The range of measurement of the flow meter is between 30-50 lit/min and its accuracy is ± 1 lit/min. This flow meter was designed to measure the volume flow rate at normal conditions (20 °C and 0.3 kgf/cm² gage), so this volume flow rate has to be changed according to actual conditions in the laboratory using Equation (2). Finally, the heated air was exhausted to the atmosphere.

$$F = F' \sqrt{\frac{T_s \cdot P_a}{T_a \cdot P_s}} \quad (2)$$

Some of the important characteristics include physical properties and geometrical dimensions of the apparatus were summarized in Table 2.

Calculation of Heat Transfer Coefficient: The heat transfer between tube and fluid flowing inside the tube can be calculated as:

$$q_w = h_i(T_w - T_b) \quad (3)$$

Temperature of the fluid flowing inside the tube is accordant to the wall temperature. Bulk temperature means an average fluid temperature and can be calculated as follow:

$$T_b = \frac{\int \rho_w C_p T dA}{\int \rho_w C_p dA} \quad (4)$$

If the fluid properties are constant, the equation reduces to

$$T_b = \frac{\int T dA}{\int dA} \quad (5)$$

From an energy balance on a section of the tube, one can determine how the change in the downstream direction

$$\int r_w C_p T dA - \left[\int r_w C_p T dA + \frac{\partial}{\partial x} \int r_w C_p T dA dz \right] + q_w \pi d_w dz = 0 \quad (6)$$

but

$$\int r_w dA = \pi d_w L \quad (7)$$

Therefore,

$$\frac{\partial T_b}{\partial z} = \frac{q_w \pi d_w}{C_p \dot{m}} \quad (8)$$

Since all quantities on the right of the above equation are constant, it can be seen that T_b is linear with x , in other words:

$$\frac{\partial T_b}{\partial z} = \text{const.} \quad (9)$$

For bulk temperature, T_b , integrate Equation (8)

$$T_b(i) = T_{in} + \frac{q_w \pi d_w}{m C_p} z \quad (10)$$

where x is distance from starting point of ohmic heating on tube.

Inside wall temperature of the tube is calculated by outside wall temperature of tube considering cylindrical wall thermal resistance according to the following relation:

$$T_w(i) = T_o(i) - q_w \left[\frac{\ln\left(\frac{D_w}{d_w}\right)}{2\pi k L} \right] \quad (11)$$

where L is the cylindrical wall thickness.

The heat flux can also be calculated as the ratio of heater power to the heating area.

$$q_w = \frac{VI}{\pi d_w Z} \quad (12)$$

From above, local heat transfer coefficient can be calculated.

$$h_i = \frac{q_w}{T_w(i) - T_b(i)} \quad (13)$$

Consequently, local Nusselt number is calculated according to:

$$Nu_i = \frac{h_i d_w}{k} \quad (14)$$

For gases both the density and the transport properties are, at least approximately, proportional to the absolute temperature of the gas raised to some power. The ratio of the absolute temperature of the wall and of the gas (e.g. bulk temperature), is therefore a good indication of whether the property variation is significant or not. As mentioned by Worsoe-Schmidt and Leppert [8], when this ratio is less than approximately 1.2, constant-properties assumptions will give reasonably accurate results for the heat transfer. Therefore, in this study all the air properties were evaluated at the mean film temperature as reported by Bejan [9].

$$T_f(i) = \frac{T_w(i) + T_b(i)}{2} \quad (15)$$

where $T_f(i)$ is the local film temperature of the air.

The average values of Nusselt number ($Nu_{ave.}$) can be calculated based on the local Nu numbers as follows:

$$Nu_{ave.} = \frac{1}{L} \int_0^L Nu_i dz \quad (16)$$

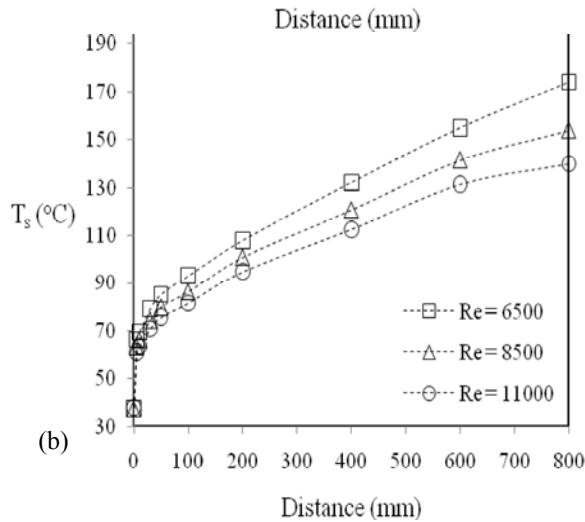
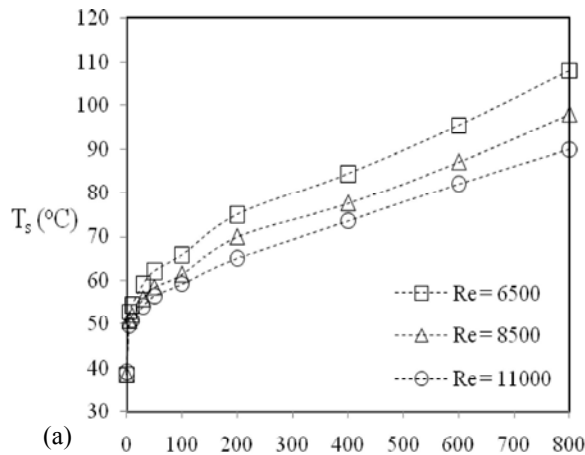


Fig. 2: Variation of surface temperature along the tube length as a function of Re
(a) at 1300 W/m² (b) at 3000 W/m²

RESULTS AND DISCUSSIONS

The effects of heating on the surface temperature, local and average Nusselt numbers in the entrance sections are presented and discussed in this section. Heat flux is varied in two levels including 1300 W/m² and 3000 W/m² and Reynolds number is varied in the range of 6500 to 11000. The surface temperature distribution for selected runs is plotted in Figure 2 at different Re numbers. As can be seen in this Figure, the surface temperature increases from a certain value with tube distance since at the tube entrance, the thickness of the boundary layer is zero. Then, it gradually increases until maximum value when the boundary layer fills the tube. It seems that in the present investigation, flow can not be developed completely and longer tube should be provided for this purpose.

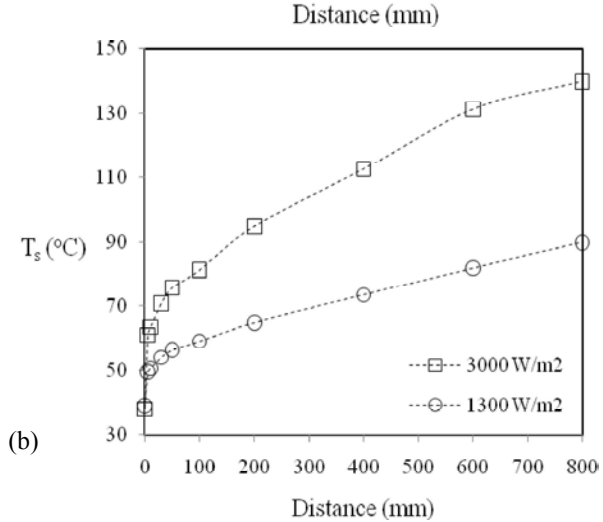
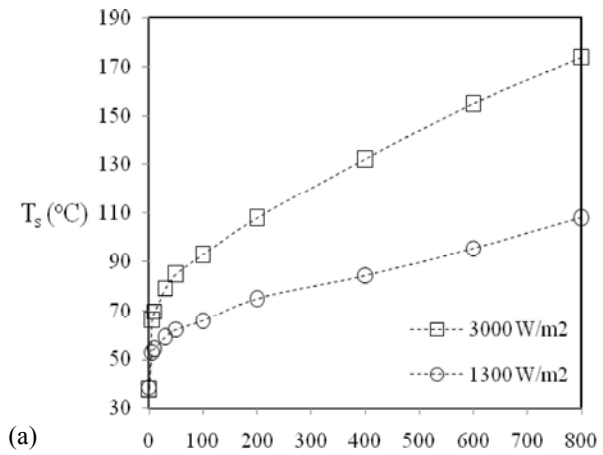


Fig. 3: Variation of surface temperature along the tube length at two different heat fluxes for
(a) Re = 6500 and (b) Re = 11000

It was already investigated that in the 3 mm inside diameter tube, the length of 68 cm is required for air to create developed flow [10]. By comparison, in the present tube with 5 mm inside diameter, longer tube (probably greater than 1 m) is needed for air flow to be developed. Therefore, all the experiments performed in this study are in developing flow condition. This point was already shown by Faris and Viskanta [2] that for a uniform wall heat flux boundary condition; fully developed heat transfer is reached asymptotically after a considerable starting length. For example, $x/d_w > 700$ was needed to establish fully developed heat transfer for water as compared to $x/d_w = 180$ for air. Furthermore, it is clear from Figure 2 that the addition of air flow rate or Re in the tube causes the surface temperature of the tube being decreased at constant heat flux condition.

This effect may be explained in terms of turbulent mixing of boundary layer at higher Re numbers.

Figure 3 show the effect of heat flux variation on the tube surface temperature for $Re = 6500$ in Figure 3 (a) and for $Re = 11000$ in Figure 3 (b). These Figures reveal also the same foregoing trend mentioned for Figures 2 and 3 that the surface temperature increases with the distance from the tube entrance.

The distribution of the local Nusselt number with the axial distance is plotted for selected runs as shown in Figures 4 and 5. The general variation of local Nu number reveals that it is of high value near the inlet of the tube because the thickness of the thermal boundary layer is zero and it decreases continuously due to the thermal boundary layer that develops.

Figure 4 (a) and (b) show the effect of the heat flux variation on the local Nu distribution for $Re=6500$ and $Re=11000$, respectively. It is apparent from this Figure that at higher heat flux, the results of local Nu number were slightly higher than the results of lower heat flux. This may be attributed to the secondary flow superimposed on the forced flow in which the effect increases as the heat flux increases leading to higher heat transfer coefficient, also due to the free convection currents domination on the heat transfer process.

It was noted that the local Nu number increases with the increasing of Re number. As the surface-to-bulk temperature difference increases, free convection becomes significant and Nu starts increasing with axial distance. This is a logical behavior since the impact of free convection is expected to be stronger for slower flows. As the Re number decreased, the buoyancy force is expected to be stronger which improves the heat transfer results. It is necessary to mention that in horizontal tube the forces of free and forced convection are perpendicular to each other resulting in the loss of rotational symmetry and the effect of secondary flow is high, hence at low Re number and high heat flux, situation makes the free convection predominant. Therefore, as the heat flux increases, the fluid near the wall becomes warmer and lighter than the bulk fluid in the core. As a consequence, two upward currents flow along the sides' walls and by continuity, the fluid near the tube center flows downstream. This sets up two longitudinal vortices, which are symmetrical about a vertical plane. These vortices reduces the temperature difference between the tube surface and the air flow which led to increase in growth of the thermal boundary layer along the tube and caused an improvement in the heat transfer results. But at low heat flux and high Re number

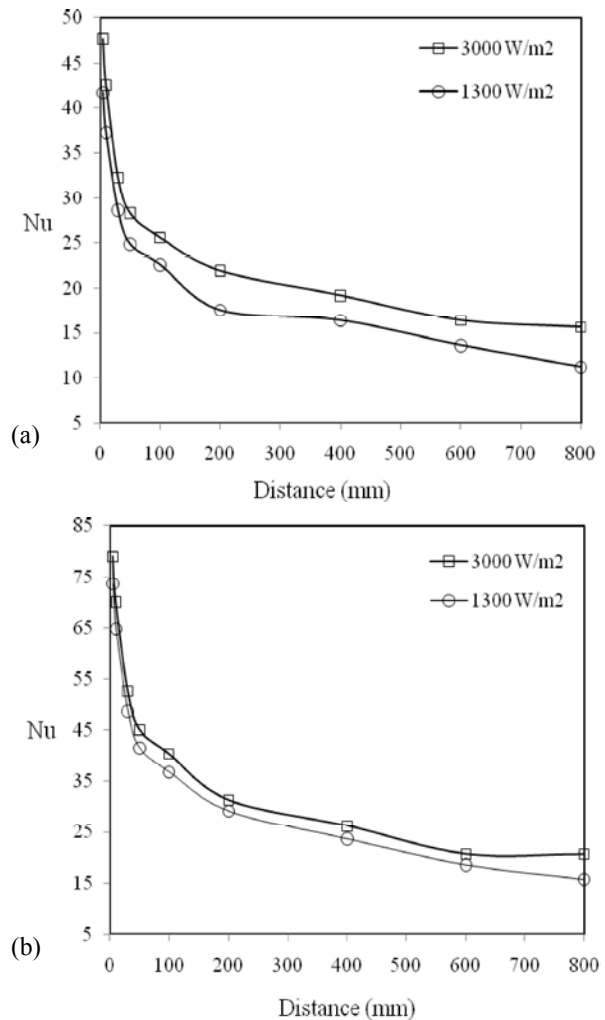


Fig. 4: Nu number variation along tube length as a function of heat flux
(a) at $Re = 6500$ and (b) at $Re = 11000$

the situation makes the forced convection predominant and the vortex strength decreases which decreases the temperature difference between the surface and the air, hence the Nu values become higher.

Figure 5 show the effect of Re number variation on the Nu number distribution, for low heat flux 1300 W/m² in Figure 5 (a) and for high heat flux 3000 W/m² in Figure 5 (b). Although the increase in Re can improve heat transfer clearly as shown in Figure 5 for both heat fluxes, comparison of these two Figures reveals that at higher heat flux the Nu distribution curves are closer to each other relative to the distribution curves at lower heat flux. It is concluded that the effect of Re is more obvious at lower heat flux in compare to higher heat flux. Whenever the free convection becomes weak, Re is the main

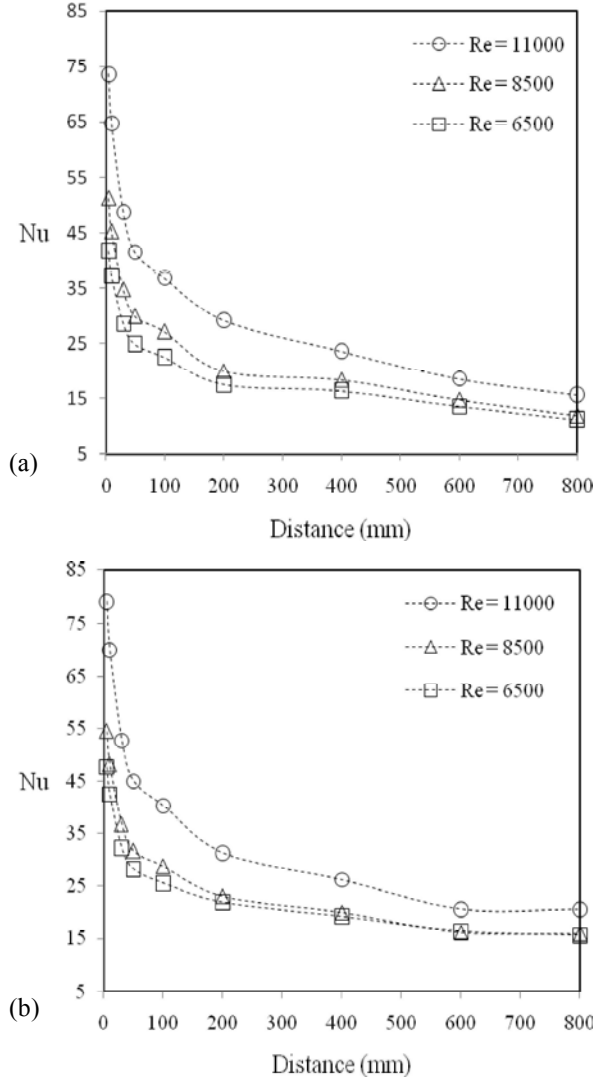


Fig. 5: Nu number variation along tube length as a function of Re number

(a) at low heat flux 1300 W/m² and

(b) at high heat flux 3000 W/m²

controller of the heat transfer and a small change in it can alter the heat transfer considerably. Alternatively, at higher heat flux the effect of free convection becomes comparable to forced convection effect and therefore Re misses its monopole controlling character. This situation can also be shown in Figure 4 where the heat flux variation changes the Nu distribution curve considerably at lower Re number.

Numerical Formulation: Simulation of mixed convection heat transfer of air in a long tube ($d_i = 0.005$ m and $Z = 0.9$ m) with uniform heat flux at the solid-gas

interface has been considered in this chapter. Fig. 1 and Table 2 show the geometry of the considered problem. The physical properties of the air are assumed to be constant except for the density in the body force, which varies linearly with the temperature (Boussinesq's hypothesis). Dissipation and pressure work are neglected. With these assumptions the dimensional conservation equations for steady state mean conditions are as follows:

Continuity equation:

$$\frac{1}{r} \frac{\partial}{\partial r}(\rho r v) + \frac{1}{r} \frac{\partial}{\partial \theta}(\rho u) + \frac{\partial}{\partial z}(\rho w) = 0 \quad (17)$$

Momentum equation:

θ -component:

$$\begin{aligned} & \frac{1}{r} \frac{\partial}{\partial r}(\rho r v u) + \frac{1}{r} \frac{\partial}{\partial \theta}(\rho u^2) + \frac{\partial}{\partial z}(\rho w u) + \frac{1}{r}(\rho u v) \\ &= -\frac{1}{r} \frac{\partial P}{\partial \theta} + \frac{1}{r^2} \frac{\partial}{\partial \theta} \left(\mu \frac{\partial u}{\partial \theta} \right) + \frac{\partial}{\partial r} \left(\frac{\mu}{r} \frac{\partial (r u)}{\partial r} \right) + \frac{2\mu}{r^2} \frac{\partial v}{\partial \theta} + \rho g \beta (T_w - T) \end{aligned} \quad (18)$$

r -component:

$$\begin{aligned} & \frac{1}{r} \frac{\partial}{\partial \theta}(\rho v u) + \frac{1}{r} \frac{\partial}{\partial r}(\rho r v^2) + \frac{\partial}{\partial z}(\rho w u) - \frac{1}{r}(\rho u^2) \\ &= -\frac{1}{r} \frac{\partial P}{\partial r} + \frac{1}{r^2} \frac{\partial}{\partial \theta} \left(\mu \frac{\partial v}{\partial \theta} \right) + \frac{\partial}{\partial r} \left(\frac{\mu}{r} \frac{\partial (r v)}{\partial r} \right) - \frac{2\mu}{r^2} \frac{\partial u}{\partial \theta} + \rho g \beta (T_w - T) \end{aligned} \quad (19)$$

z -component:

$$\frac{1}{r} \frac{\partial}{\partial r}(\rho r v w) + \frac{\partial}{\partial z}(\rho w^2) = -\frac{\partial P}{\partial z} + \frac{1}{r^2} \frac{\partial}{\partial \theta} \left(\mu \frac{\partial w}{\partial \theta} \right) + \frac{1}{r} \frac{\partial}{\partial r} \left(\mu r \frac{\partial w}{\partial r} \right) - \rho g (T_w - T) \quad (20)$$

Energy equation:

$$\frac{1}{r} \frac{\partial}{\partial \theta}(\rho u T) + \frac{1}{r} \frac{\partial}{\partial r}(\rho r v T) + \frac{\partial}{\partial z}(\rho w T) = \frac{1}{r^2} \frac{\partial}{\partial \theta} \left(\frac{k}{C_p} \frac{\partial T}{\partial \theta} \right) + \frac{1}{r} \frac{\partial}{\partial r} \left(\frac{k}{C_p} \frac{\partial T}{\partial r} \right) \quad (21)$$

This set of nonlinear elliptical governing equations has been solved subject to following boundary conditions:

- At the tube inlet ($z = 0$):

$$w = w_0, \quad u = v = 0, \quad T = T_0 \quad (22)$$

- At the gas-solid interface:

$$w = u = v = 0, \quad q = -k \frac{\partial T}{\partial r} \quad (23)$$

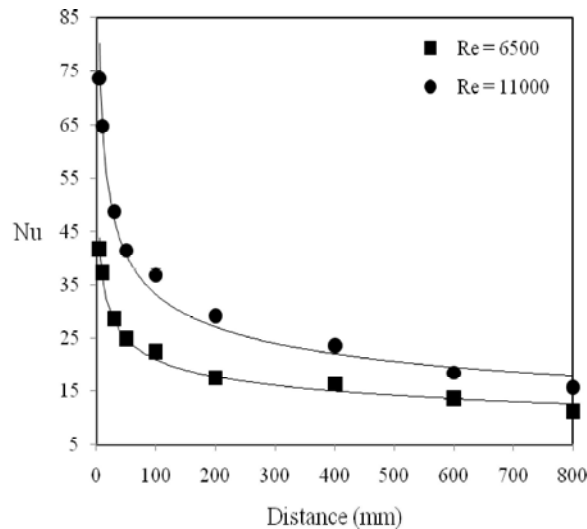


Fig. 6: The comparison of experimental Nu number and the prediction of numerical formulation

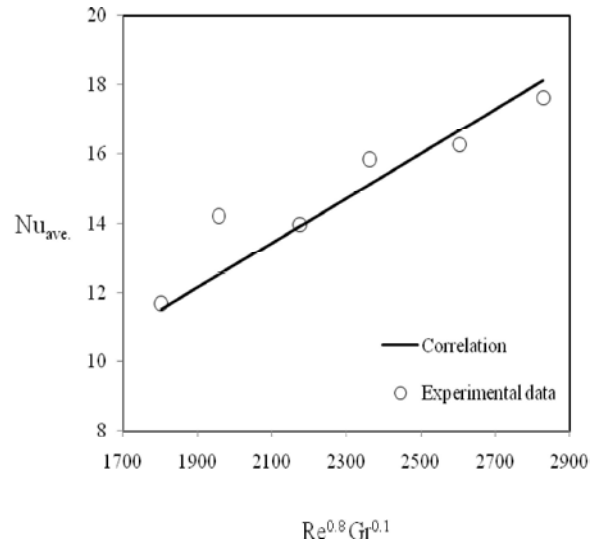


Fig. 7: Comparison between experimental $Nu_{ave.}$ and the suggested correlation

- At horizontal symmetry plane

$$\theta = 0, \theta = \pi, u = 0, \frac{\partial T}{\partial \theta} = \frac{\partial w}{\partial \theta} = \frac{\partial v}{\partial \theta} = 0 \quad (24)$$

- At the tube outlet, the diffusion flux in the direction normal to exit plane is assumed to be zero for all variables and an overall mass balance correction is applied.

The results of simulation and also the experimental data are shown in Fig. 6 for the sake of comparison. As can be seen in Fig. 6 the numerical formulation of the problem gives a result which is in good agreement with the experimental data over the length of the tube. Also, it is clear that this mathematical model can predict the effect of secondary flow with acceptable accuracy.

Correlation of the Experimental Data: The average Nusselt numbers, resulted from all the experiments performed in this work, were correlated in terms of the relevant parameters with an empirical equation for a horizontal tube and were presented in Figure 7. As explained in the previous sections, Re and Gr are the main dimensionless numbers which account for considerable contribution of forced and free convections in this study. It was proposed by the authors that the heat transfer equation has this form:

$$Nu_{ave.} = a Re^b Gr^c \quad (25)$$

Using three dimensional curve fitting to the data, three constants of Equation (25) were determined and the suggested correlation, as shown in Equation (26) can reproduce the average Nusselt number with absolute average error of less than 4%. The slope of the straight fitted line in Figure 6 indicates the constant “a” in the suggested correlation.

$$Nu_{ave.} = 0.0064 Re^{0.8} Gr^{0.1} \quad (26)$$

CONCLUSIONS

Turbulent air flow mixed convection heat transfer in the thermal entry region of a horizontal tube with constant wall heat flux has been experimentally studied. It was found that the surface temperature is higher for low Re number than for high Re number due to the free convection domination on the combined heat transfer process. This consequently makes the local Nu numbers to be higher for high Re number than for low Re number due to the forced convection domination on the heat transfer process. The effect of secondary flow due to the buoyancy forces was found to be significant at higher heat flux and lower flow rate. Finally, the average Nu numbers were correlated in terms of the relevant dimensionless parameters with an empirical correlation evidencing an overall accuracy of the order of $\pm 4\%$.

ACKNOWLEDGMENT

The author gratefully acknowledge the financial support provided by Islamic Azad University, Mahshahr branch, Iran to perform research project entitled: "Experimental study of forced convection heat transfer coefficient and Nusselt number to air in a tube".

NOMENCLATURE

A	Cross sectional area of the tube	[m ²]
C _p	Specific heat at constant pressure	[J/kg K]
D _w	Tube outer diameter	[m]
d _w	Tube inner diameter	[m]
F	Volume flow rate at actual condition	[m ³ /s]
F'	Volume flow rate at standard condition	[m ³ /s]
h _i	Local heat transfer coefficient	[W/m ² K]
k	Thermal conductivity of tube	[W/m °C]
L	Thickness of tube	[m]
\dot{m}	Flow rate of air	[kg/h]
P _a	Actual pressure at flow meter	[kgf/cm ²]
P _s	Standard pressure = 1.333	[kgf/cm ²]
q	Power	[W]
q _w	Heat flux per unit inner wall area of tube	[W/m ²]
T _a	Actual temperature at flow meter	[K]
T _b	Bulk temperature of fluid	[K]
T _f	Film temperature according to Equation (15)	[K]
T _{in}	Inlet temperature of air flow	[K]
T _o	Outside wall temperature of tube	[K]
T _s	Standard absolute temperature = 293	[K]
T _w	Inside wall temperature of tube	[K]
u	Fluid velocity in radial direction	[m/s]
v	Fluid velocity in circumferential direction	[m/s]
w	Fluid velocity in axial direction	[m/s]
Z	Tube length	[m]
z	Distance from starting point of ohmic heating on tube	[m]

Dimensionless groups:

Gr	Grashof No.	$(g\beta d_w^4 q_w / kv^2)$
Nu	Nusselt No.	(hd_w / k)
Re	Reynolds No.	(Ud_w / ν)

Greek Letters:

ρ	Fluid density	[kg/m ³]
ν	Fluid viscosity	[m ² /s]

REFERENCES

1. Ghajar, A.J. and L.M. Tam, 1994. Heat transfer measurements and correlations in the transition region for a circular tube with three different inlet configurations. *Experimental Thermal and Fluid Science*, 8: 79-90.
2. Faris, G.N. and R. Viskanta, 1969. An analysis of laminar combined forced and free convection heat transfer in a horizontal tube. *International Journal of Heat and Mass Transfer*, 12: 1295-1309.
3. Tam, L.M. and A.J. Ghajar, 1998. The unusual behavior of local heat transfer coefficient in a circular tube with a bell-mouth inlet. *Experimental Thermal and Fluid Science*, 16: 187-194.
4. Mori, Y., K. Futagami, S. Tokuda and M. Nakumara, 1966. Forced convection heat transfer in uniformly heated horizontal tube-experimental study on the effect of buoyancy. *International Journal of Heat and Mass Transfer*, 9: 453-463.
5. Kupper, A., E.G. Hauptmann and M. Iqbal, 1969. Combined free and forced convection in a horizontal tube under uniform heat flux. *Sol. Energy*, 12(4): 439-446.
6. Lei, Q.M. and A.C. Trupp, 1991. Experimental study of laminar mixed convection in the entrance region of a horizontal semicircular duct. *International Journal of Heat and Mass Transfer*, 34(9): 2361-2372.
7. Mohammed, H.A., A. Campo and R. Saidur, 2010. Experimental study of forced and free convective heat transfer in the thermal entry region of horizontal concentric annuli. *International Communications in Heat and Mass Transfer*, 37(7): 739-747.
8. Worsoe-Schmidt, P.M. and G. Leppert, 1965. Heat transfer and friction for laminar flow of gas in a circular tube at high heating rate, solutions for hydrodynamically developed flow by a finite-difference method. *International Journal of Heat and Mass Transfer*, 8: 1281-1301.
9. Bejan, A., 1984. *Convective Heat Transfer*. (1st edition). John Wiley and Sons Inc., New York, Chaps, pp: 2-4.
10. Mohammed, H.A. and Y.K. Salman, 2007. The effects of different entrance sections lengths and heating on free and forced convective heat transfer inside a horizontal circular tube. *International Communications in Heat and Mass Transfer*, 34: 769-784.